ISSN: 0067-2904

Determination of the Dispersion Profile in Photonic Crystal Fibers using the Empirical Relationship

Marwan Hafeedh Younus*, Odai Falah Ameen, Muayad Abdullah Ahmed,Yaser Yahya Kassim

Department of Physics, College of Education for Pure Science, University of Mosul, Mosul, Iraq

Received: 21/11/2023 Accepted: 4/9/2024 Published: 15/2/2025

Abstract

In this work, a single-mode endless photonic crystal fiber (PCF) is proposed and theoretically analysed using the empirical relationship method. The designed PCFs are composed of three uniform rings of air holes arranged in a circular shape. Three samples of fibers ($PCFs_{Pure}$, $PCFs_{doped1}$ and $PCFs_{doped2}$) with the same structure but are only different in the material of core have been investigated. The guiding properties of PCFs are studied in terms of effective refractive index, confinement loss and dispersion profile. The numerical results show that the $PCFs_{doped2}$ exhibits good properties such as high refractive index, low confinement loss and red shifting in the zero dispersion compared to other samples. A red shifting in the zero dispersion, achieved in this study, may be important to generate the soliton fission. Moreover, all the designed PCFs perform a negative dispersion at higher d/Λ, which are used to obtain the coherence supercontinuum generation spectrum. The designed PCFs in this study can be used in the transmission of optical signals using different types of materials in the core structure of PCFs.

Keywords: Photonic crystal fiber**,** Zero dispersion, Shiftting dispersion, Effective refractive index, The effective area.

تحديد شكل التشتت في ألياف البلورة الضوئية باستخدام العلاقة التجريبية

مروان حفيظ يونس*، عدي فلاح امين، مؤيد عبدالله احمد ، ياسر يحيى قاسم

قسم الفيزياء, كلية التربية للعلوم الصرفة, جامعة الموصل, نينوى, العراق

الخلاصة

في هذا العمل، تم اقتراح ألياف بلورية فوتونية احادية النمط (PCFs) وتحليلها نظريا باستخدام طريقة العلاقة التجريبية. تتكون PCFs المصممة من ثلاث حلقات منتظمة من فتحات الهواء مرتبة على شكل دائري. تم فحص ثلاث عينات من الألياف ($PCFs_{Pure}$، $PCFs_{doped1}$ و$PCFs_{doped2}$) بنفس الطريقة ولكنها تختلف فقط في مادة قلب الليف. تمت دراسة الخصائص التوجيهية لمركبات PCF من حيث معامل الانكسار الفعال، خسائر الحصر وايضا دراسة شكل التشتت. أظهرت النتائج أن $PCFs_{doped2}$ يظهر خواص جيدة مثل معامل الانكسار العالي، خسائر حصر قليلة و انتقال في التشتت الصفري باتجاه الاطوال الموجية الحمراء مقارنة بالالياف الأخرى. قد يكون الانتقال نحو المنطقة الحمراء للتشتت الصفري الذي تم الحصول عليه في هذه الدراسة مهمًا لتوليد موجة السوليتون. من جانب اخر، فإن جميع مركبات PCF

*Email: marwan.hafed@uomosul.edu.iq

المصممة تمتلك تشتتًا سلبيًا عند قيم عالية للنسبة d/Λ والتي تستخدم للحصول على طيف توليد الاستمرارية الفائقة. علاوة على ذلك، يمكن استخدام الالياف البلورية الضوئية المصممة في هذه الدراسة بشكل فعال في نقل الإشارة الضوئية من خلال اختيار أنواع مختلفة من المواد في قلب الليف.

الكلمات المفتاحية: الالياف البورية الفوتونية، التشتت الصفري، معامل الانكسار الفعال

1. Introduction

The photonic crystals have very important applications; one is designing novel waveguides such as Photonic Crystal Fibres (PCFs) and holey fibres (HFs) [1-4], which can be considered as the-state-of-the art of the fibres. In the PCFs, the cladding region consists of an array of air holes arranged in a regular triangular lattice [4-6]. The PCFs have remarkable properties compared with traditional optical fibres. One of these properties is that PCFs are produced mainly from silica glass (SiO_2) surrounded by an array of microscopic air channels extending along their length [7-9]. In addition, the PCFs based on index-guiding are formed by a discontinuity in the refractive index or the defect, which can be made by missing one air hole or more in the PCF central to form a solid core. In addition, the guided light within the PCFs propagates between the core and the cladding via total internal reflection (TIR) [10-13]. During the past few years, two main groups have reported many studies about the PCFs. The first group used several methods to model and study the propagation properties of the PCFs. These methods include plane wave expansion, multipole, finite difference, and finite element methods. The other group has used empirical relationships to study and model the PCFs [14-18]. The main advantage of the empirical relationships over the other methods is that it is less costly and require less computational time to model the PCFs.

Due to the structure of the PCFs, researchers have been interested in studying the influence of the parameters of PCF structure, such as the diameter of holes (d), pitch size (ʌ), number of air holes (Nr), and number of missing holes (NMr), on the dispersion profile. By varying these parameters, the profile of dispersion can be obtained, such as zero [19], nearly zero ultra-flattened [20], flattened [10] and shifting dispersions [21].

This study aims to design an endless single-mode, Solid Core Photonic Crystal Fibre (SCPCF), which consists of three uniform rings from air holes in a circular shape using the empirical relationship method. The structures of the PCFs were designed using a simple method without any complexity. The structure property of the SCPCF was studied for three samples of solid-core photonic crystal fibers, PCFs, PCFs (doped1) and PCFs (doped 2), of the same parameters but of different core materials. The aim is to enhance the properties of the designed PCFs parameters, which can easily be evaluated without complex computations or numerical calculations.

2. The Design of Solid Core Crystal Fibre (SCPCF)

In conventional PCFs, the cladding structure is typically formed with the same diameter as the air holes but in different lattice shapes (square, hexagonal and circular). The dispersion profile can be designed by changing the hole diameter, the hole-to-hole spacing (pitch size), the diameter of the core (*D*), the number of rings (*Nr*), the number of missing holes (*MNr*), and the material of the core. An index of guiding PCFs is to contain a missing air hole at the centre, which acts as the fiber core. As the lattice periodicity of the cladding is critical to confine the light into the high index core region, an index guiding PCF with a high refractive index core was suggested to enhance the dispersion profile in a wide range of wavelengths. The cross-section of the structure geometry, electric field distribution and light confinement for the designed PCF are shown in Figure 1, which demonstrates the electric field confined

in the core of the PCF. In the PCF cladding, three rings with 60 air holes are arranged uniformly in a circular manner. The centre-to-centre space between the adjacent holes was denoted as the pitch size (Λ) and (d) the diameter of the air hole. A waveguide core was formed by a single missing air hole, which constitutes a defect region in the photonic crystal material. To illustrate how the dispersion profile was affected by tuning the material of the core for a given diameter of hole and pitch size along a range of wavelengths, three SCPCFs were considered in this work which have the following parameters: core diameter (D) of 1.4 µm, air hole diameter (d) of 0.4µm, different pitch sizes (Λ) of 1, 1.14, and 1.33, different air filling factors (d/Λ) of 0.3, 0.35, and 0.4, different number of air holes (Nr) of 1, 2, and 3, and number of missing holes (NMr) of 1. Our PCF was formed of circular rings of air holes implanted in different materials background matrices. These three background materials were used as the core materials: pure SiO_2, (9.1 mol. P_2O_5, 90.9 mol SiO_2) referred to as doped 1 and (8.9 m/o Na_2O, 32.5 m/o B_2O_3 + 50.6 mol SiO_2) referred to as doped 2; keeping the holes of cladding completely hollow. The refractive index of the designed PCF obeys Sellmeier equation. To confine and guide the light within the fibre core, the refractive index of the core should be greater than the effective refractive index of the guided fundamental mode. For the designed PCFs, the distribution of the infinite periodic array of the air holes that embedded into the background material of the fibre acts as the effective refractive index of the clad. The diameter of the hole and air filling factor d/Λ were carefully chosen for designing a simple structure, which satisfied the light guiding conditions and offered a wide range of operating wavelengths guidance of fundamental mode over the solid core of the PCFs.

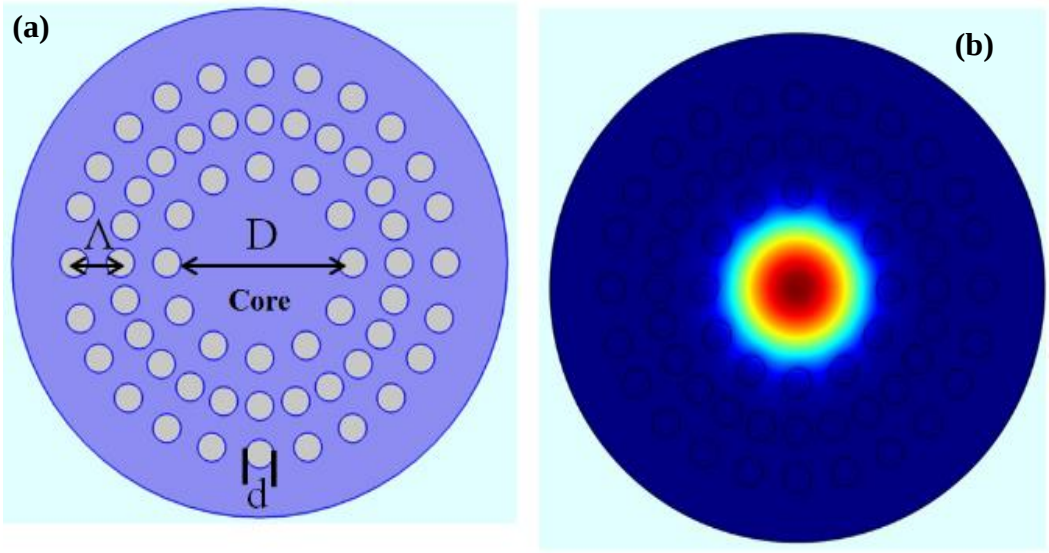

Figure 1: (a) Cross section geometry of the PCFs, (b) Electric field for three circular rings.

Theoretical Structure of PCFs

Three photonic crystal fibres were designed with circular structures using the empirical relationship method. The aim was to examine the behaviour of the designed PCFs with different core materials (background material); $PCFs_{pure}$, $PCFs_{doped.1}$ and $PCFs_{doped.2}$. Three layers of air holes guided the light in the region of the core. At first, the required values were empirically extracted. Then, the effective refractive index (RI) values were calculated. The final step involved plotting the graphs of the different optical properties, refractive index, confinement loss, and zero dispersion under wavelength range from 0.5 µm to 2 µm. Our designed PCFs were studied for the same air hole diameter. In the single mode silica photonic

crystal fiber, the chromatic dispersion (*D*) can be calculated by the summation of material dispersion (*Dm*) and waveguide dispersion (*Dw*) [15, 22], which is given by[17]:

$$D(\lambda) = -\frac{\lambda}{c}\frac{\partial^2 \mathrm{Re}(n_{eff})}{\partial^2 \lambda} + D_m \tag{1}$$

Where: λ and *c* are the wavelength and the light speed in vacuum, respectively. PCF is generally described in terms of normalized frequency (*V*) which is given by [17, 18, 23]:

$$V_{PCFs} = [u^2 + w^2]^{\frac{1}{2}} \tag{2}$$

Where: *u* is the normalized transverse phase and *w* is the attenuation constant and can be given as [17, 24]:

$$\frac{2\pi a}{\lambda} U = [\mathrm{n}^2_{core}(\lambda) - \mathrm{n}^2_{eff}(\lambda)]^{\frac{1}{2}} \tag{3}$$

$$\frac{2\pi a_{eff}}{\lambda} W = [n^2_{eff}(\lambda) - n^2_{FSM}(\lambda)]^{\frac{1}{2}} \tag{4}$$

n_{core} and n_{FSM} are indices of the core and the cladding, respectively, n_{eff} represents the effective refractive index of the fundamental mode, and a_{eff} is the effective radius of the core which is assumed to be $\Lambda/3$. The effective *V* parameter for the PCFs is written as[17, 24]:

$$\frac{2\pi a_{eff}}{\lambda} V_{eff} = [n^2_{core}(\lambda) - n^2_{FSM}(\lambda)]^{\frac{1}{2}} \tag{5}$$

and the n_{FSM} is given by:

$$n_{FSM} = \frac{2\pi a_{eff}}{V_{PCF}\lambda}[n^2_{core}(\lambda) - 2]^{\frac{1}{2}} \tag{6}$$

It should be noted that V_{PCF} value is calculated as a function of both d/Λ and λ/Λ, and can be written as [17, 24]:

$$V_{PCF} = A_1 + \frac{A_2}{1 + A_3 \exp(A_4 \frac{\lambda}{\Lambda})} \tag{7}$$

here, *Ai* (i = 1 to 4) is the fitting parameter that depends on d/Λ; it can be described by the following equation [17]:

$$A_i = b_{i0} + [\mathrm{b}_{i1}]^{ai1} + [b_{i2}]^{ai2} + [b_{i3}]^{ai3} \tag{8}$$

The fitting coefficients values of *b* and *a* are presented in Table 1 [17].

Table 1 : The values of fitting coefficients.[1]

	i=1	**i=2**	**i=3**	**i=4**
b_{i0}	**54.808 * 10^{-2}**	**71.041* 10^{-2}**	**16.904* 10^{-2}**	**-152.736* 10^{-2}**
b_{i1}	**500.401* 10^{-2}**	**185.765* 10^{-2}**	**185.765* 10^{-2}**	**106.745* 10^{-2}**
b_{i2}	**-1043.248* 10^{-2}**	**4741.496* 10^{-2}**	**1896.849* 10^{-2}**	**193.229* 10^{-2}**
b_{i3}	**822.992* 10^{-2}**	**-43750.962* 10^{-2}**	**-4243.18* 10^{-2}**	**389* 10^{-2}**
a_{i1}	**500* 10^{-2}**	**180* 10^{-2}**	**170* 10^{-2}**	**-84* 10^{-2}**
a_{i2}	**700* 10^{-2}**	**732* 10^{-2}**	**1000* 10^{-2}**	**102* 10^{-2}**
a_{i3}	**900* 10^{-2}**	**2280* 10^{-2}**	**1400* 10^{-2}**	**1340* 10^{-2}**

Substituting Equations 7 and 8 in Equation 6 gives the values of n_{FSM}. The effective refractive index can be obtained by:

$$n_{eff} = [n_{FSM}^2(\lambda) + (\frac{W\lambda}{2\pi a_{eff}})^2]^{\frac{1}{2}} \quad (9)$$

where W is given by:

$$W = B_1 + \frac{B_2}{1 + B_3 \exp(B_4 \frac{\lambda}{\Lambda})} \quad (10)$$

Bi (i = 1 to 4) are the fitting parameters and depend on d/Λ. Bi can be calculated by the following expression [17]:-

$$B_i = d_{i0} + d_{i1}[\frac{c}{\Lambda}]^{c_{i1}} + d_{i2}[\frac{c}{\Lambda}]^{c2} + d_{i3}[\frac{c}{\Lambda}]^{c_{i3}} \quad (11)$$

The coefficients d_{i0} to d_{i3} and c_{i1} to c_{i3} were given by Saitoh and Koshiba [17]. Substituting Equations (6,10 and 11) in Equation (9), the relation for the refractive index in terms of the main geometrical parameters of the fiber is obtained. Additionally, the refractive index of the core can be calculated using Sellmeier equation:

$$n_{core}^2(\lambda) = 1 + \sum_{i=1}^{3} \frac{A_i \lambda^2}{\lambda^2 - \lambda_i^2} \quad (12)$$

Where: Ai (1,2,3) and λ_i (1,2,3) are coefficients related to material oscillator strength and oscillator wavelengths, respectively (see Table 2). The values of these coefficients, for pure silica and other doped glass are obtained empirically by Sellmeier equation. These values are shown in Table 2 [25, 26]. Using 'n_{eff}', the other parameters such as confinement loss, effective area and dispersion parameter can be calculated.

Table 2: Sellmeier constants for pure Silica and doped glass [24,25].

	SiO_2	9.1m/oP_2O_5,90.9m/o SiO_2	(8.9 m/o Na_2O, 32.5m/o B_2O_3,+50.6 m/o SiO_2
A_1	0.6961663	0.695790	0.796468
A_2	0.4079426	0.452497	0.497614
A_3	0.8974794	0.712513	0.358924
λ_1	0.0680430	0.061568	0.094359
λ_2	0.1162414	0.119921	0.093386
λ_3	9.896161	8.656641	5.999652

The propagation constant (β) of the electromagnetic wave is the amount of the variation undergone by the wave amplitude propagating in a given direction. It is obtained from the imaginary part of the refractive index. The propagation constant β is calculated by following equation[14]:

$$\beta = n_{eff} \frac{2\pi}{\lambda} \tag{13}$$

3. Confinement Loss and Effective Mode Area

The losses in PCFs occur due to absorption, intrinsic material, imperfection in the structure, and confinement loss. The losses can be minimized by carefully enhancing the fabrication process. The confinement loss which occurs in single material fibers is defined as light leakage from the core to the clad. It is an unwanted parameter that must be reduced. In PCFs, the propagated modes inherently leak from the core to the clad of the fiber when the refractive index of the core is similar to refractive index of the cladding without holes. The confinement losses can be minimized exponentially when the number of air holes' rings is increased. It can be calculated by [27]:

$$L = 8.686 K_o I_m(n_{eff}) \tag{14}$$

Where: $K_0 = 2\pi/\lambda$ represents the free-space propagation constant and $I_m(neff)$ represents the imaginary part of the effective refractive index. The effective area (A_{eff}) is defined as the fiber area that covers the transverse dimension of the fiber. The effective area is not only a significant parameter in the nonlinearity's setting but also links to the leakage loss. A small effective area provides a high power in the core region, which is important for nonlinear effects to be significant. The effective area is calculated by the expression:

$$A_{eff} = \frac{[\int\int |E|^2 \, dxdy]^2}{\int\int |E|^4 \, dxdy} \tag{15}$$

The unit of the effective mode area (A_{eff}) is μm^2, E is the amplitude of the electric field in the medium. If the operating wavelength is given, both of the confinement loss and effective area can be controlled by choosing the pitch size, hole diameter and number of rings.

4. Results and Discussion

5.1. Calculation of the High Refractive Index of the PCFs Core

All the three-ring PCFs have the same parameters, but they only differ in the material of their cores. For these structures, the effective refractive indices are plotted against the different values of pitch size (Λ). Figure 2 shows the effective refractive index as a function of wavelength for PCF_{pure}, PCF_{doped1} and PCF_{doped2}. All PCFs are at air filling, i.e. d/Λ=0.3 for single-mode operation and d/Λ=0.35, 0.4 for multi-mode operation. It reveals that the effective refractive index decreased when the wavelength was increased because the short wavelengths propagate through the region of high refractive index, whereas the long wavelengths have stronger capacity to propagate in the region of low refractive index.

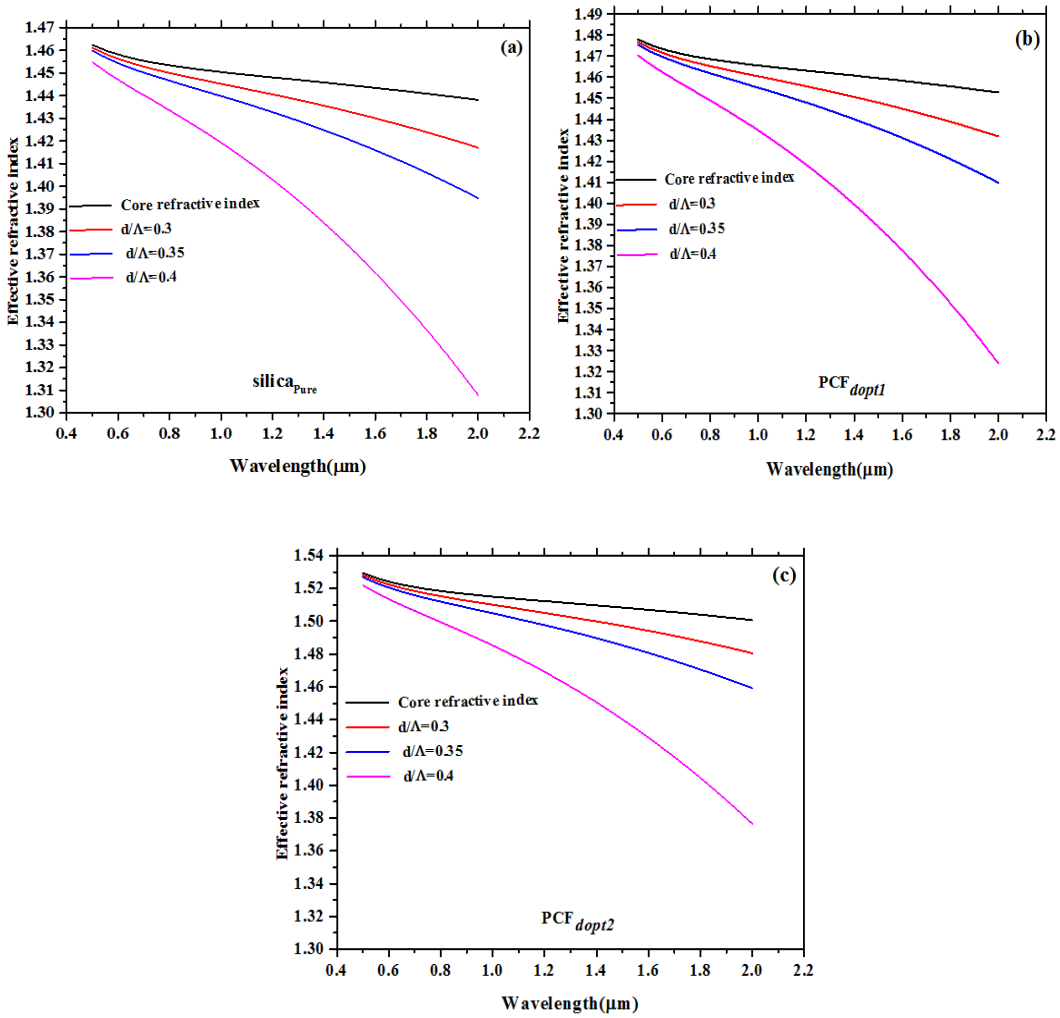

Figure 2: Effective refractive index for PCF_{pure} , PCF_{doped1} and PCF_{doped2} as a function of wavelength for different values of pitch size(Λ)

It can be noted from Figure 2 that the values of the refractive index decrease with increasing the values of air-filling factor for all the designed PCFs. There was a negligible difference in the results for short wavelengths (0.4-0.8)μm. At the long wavelengths, the difference became apparent. This is because the refractive index of a material depends strongly on wavelength. Moreover, when the spacing of the centre-to-centre of holes (Λ) was decreased, the fraction of air in the PCFs increased, so the amount of the silica or doped

silica (core material) decreased in the fiber. Thus, the refractive index decreased in the wavelength range (0.5 to 2.0)µm. From these results, it can be concluded that the effective refractive index increases by increasing the size of the hole pitch (Λ). The comparison of the effective refractive indices of the designed fibers (PCF_{pure}, PCF_{doped1} and PCF_{doped2}) at the air fraction (d/Λ=0.3) is illustrated in Figure 3. The refractive index of PCF_{doped2} is slightly higher than that of PCF_{pure} and PCF_{doped1}. Hence, the effective refractive index of the proposed PCF_{doped2} is the highest. It is worth observing here that low confinement loss is desirable for operating wavelength (0.4 µm -2.2µm) in the $PCFs_{doped2}$. This is essential to decrease the confinement losses, and may increase the confinement energy of light towards the centre of the PCFs core.

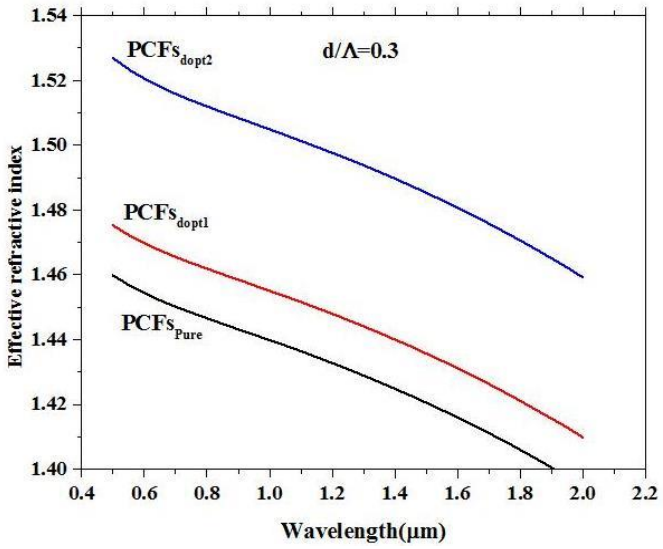

Figure 3: Comparison of effective refractive index profiles of the three designed PCFs: (PCF_{pure} , PCF_{doped1} and PCF_{doped2}) with air fraction (d/Λ =0.3).

Confinement loss represents the light leaking from the core to the clad of fiber. Figure 4 shows the confinement loss in relation to the operating wavelength of PCF_{pure}, PCF_{doped1} and PCF_{doped2}. As seen from this Figure, the confinement loss generally increased with respect to wavelength. This means that as wavelength increased, more light escaped from the fiber core to the cladding. The confinement losses of the designed PCF_{pure}, PCF_{doped1} and PCF_{doped2} at 1.5 µm are 0.878 dB/µm, 0.8748 dB/µm and 0.8676 dB/µm, respectively. The PCF_{doped2} has lower confinement loss than PCF_{pure} and PCF_{doped} because it has a higher effective refractive index. This proves that more light is confined within the core of the PCF_{doped2} due to the high refractive index, which is beneficial to propagate the signals in the fiber with low losses. Therefore, it can be said that increasing the refractive index of the core improves the confinement energy of light towards the core center of the PCFs.

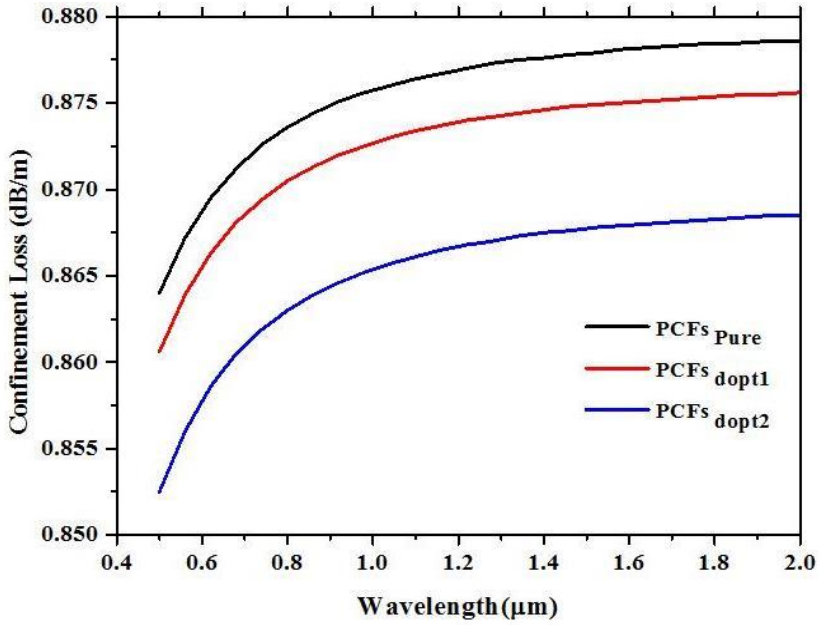

Figure 4: Confinement Loss of PCF_{pure} , PCF_{doped1} and PCF_{doped2} as a function of wavelength at air fraction(d/Λ=0.3).

5.2. Dispersion of PCFs

The dispersion parameters and zero dispersion wavelengths (ZDW) in optical communications systems play an important role in determining the information capacity carried in the optical fiber. In this work, dispersion was studied and improved with and without doped silica. The dispersion as a function of wavelength for different values of air filling factor (d/Λ=0.3, 0.35 and 0.4) is shown in Figure 5. It can be seen from Figure 5 that the shifting in the zero dispersion is toward alonger operating wavelength. Figure 5a shows that the shifting in ZDW of PCF_{pure} is from 0.74 µm to 0.88 µm, Figure 5b shows the shifting of PCF_{doped1} is from 0.75 µm to 0.935 µm and Figure 5c shows the shifting of PCF_{doped2} is from 0.797 µm to 1.034 µm. The $PCFs_{doped.2}$ structure showed good behaviour, such as shifting in zero dispersion and lower confinement losses, compared to other structures. The red shifting in the zero dispersion is important to generate the soliton fission. It can be noted that the ZDW of PCF $_{doped2}$ with a high index in the core has shifted towards longer wavelengths. Thus, the doped2 material with the high refractive index in the core is useful to shift the ZDW of the PCF towards the longer wavelength. The numerical results of the three designed PCFs are shown in Table 3.

Table 3: The numerical results of the designed PCFs for single mode and multimode operation

PCF	λ_{ZD}(µm)	*NA*	A_{eff} (µm^2)	©(m^{-1}W^{-1})
Pure	**0.74 to 0.88**	**0.1887**	**10.86**	**0.0133**
Doped 1	**0.75 to 0.935**	**0.1886**	**10.86**	**0.0133**
Doped 2	**0.797 to 1.034**	**0.191**	**10.91**	**0.0111**

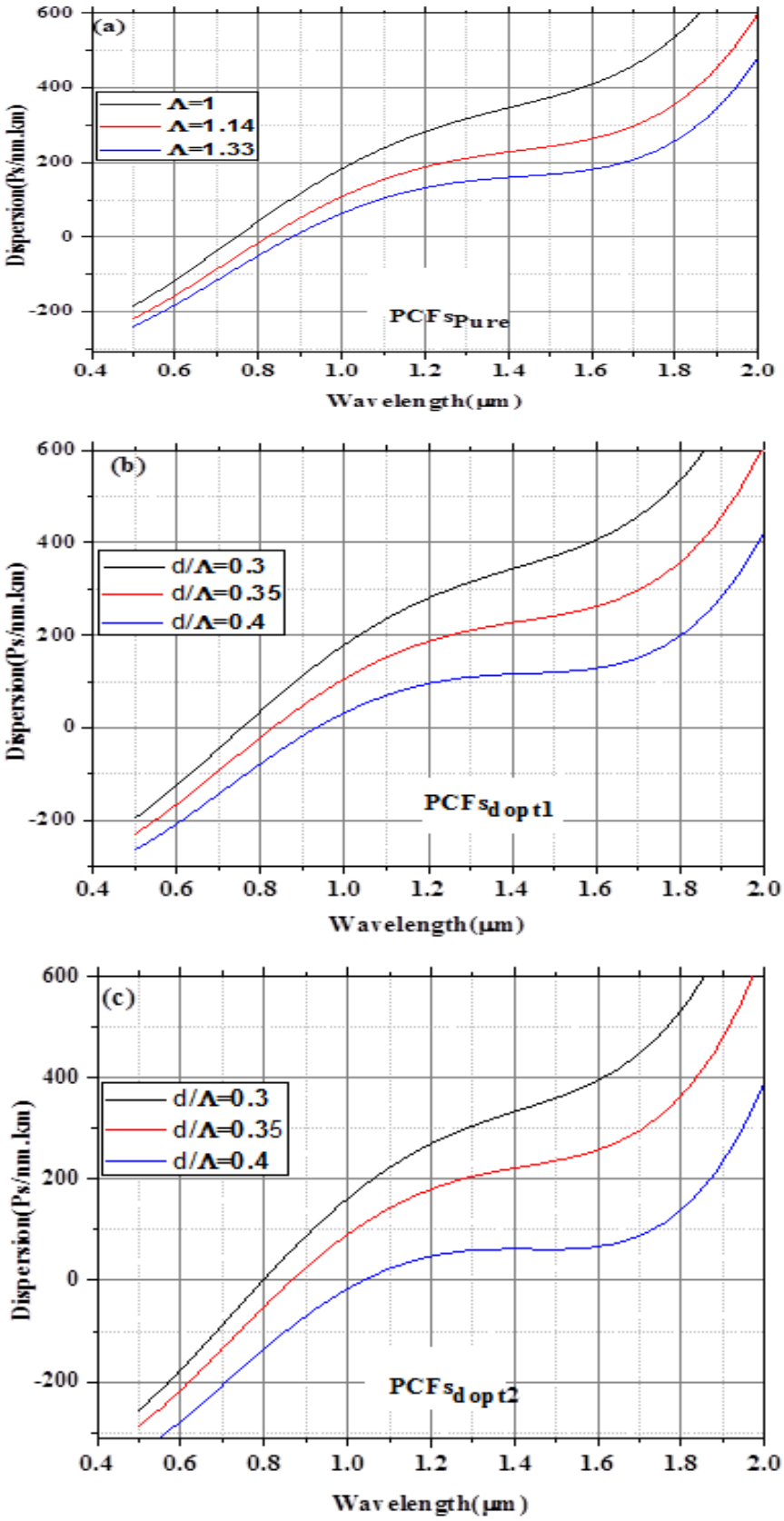

Figure 5: Dispersion profile of PCF_{pure} , PCF_{doped1} and PCF_{doped2} at different values of air fraction (d/Λ)

The dispersion profile of the PCF_{pure}, PCF_{doped1} and PCF_{doped2} at air fraction (d/Λ=0.3) were compared, as shown in Figure 6. From this figure, it is clear that the three samples of the designed PCFs have shown a shift in the ZDW. The (PCF_{pure}) illustrates the dispersion profile of Pure silica with a ZDW of 0.88 µm. The (PCF_{doped1}) is related to the dispersion profile of (9.1 m/o P_2O_5, 90.9 m/o SiO_2) with ZDW of 0.935 µm, while (PCF_{doped2}) shows the dispersion profile of (8.9m/oNa_2O, 32.5B_2O_3,+50.6SiO_2) with ZDW of 1.034 µm. Moreover, the results show the doped silica in the core, increased the large negative dispersion value at the operating wavelength. The dispersion of PCF_{doped2} compared to PCF_{pure} and PCF_{doped1} became more negative at the operating wavelength from 0.5 µm to 1.041 µm. It is important to mention that the Dispersion Compensating Fibers (DCFs) possess a negative dispersion over a wide operating wavelength range. Furthermore, a short length of a dispersion compensating fiber is required to reduce the insertion loss and decrease the cost. Nowadays, DCFs are widely used to compensate for the chromatic dispersion[27]. Additionally, the higher power spectral densities of PCFs with ZDW may be valuable in applications of super-continuum generation[18].

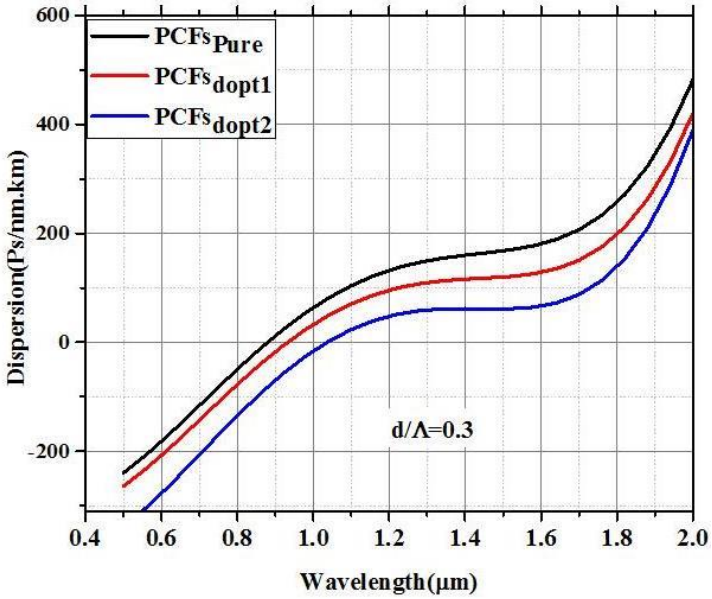

Figure 6: Dispersion profile of PCFpure, PCF_{doped1}, and PCF_{doped2} as a function of wavelength at d/Λ=0.3.

5. Conclusion

Three types of PCFs ($PCF_{pure}(SiO_2)$), PCFs($_{doped1}$) (9.1 m/o P_2O_5, 90.9 m/o SiO_2) and PCFs($_{doped2}$) (8.9 m/o Na_2O, 32.5 m/o B_2O_3 + 50.6 m/o SiO_2) were designed using the empirical relationship. The characteristics of dispersion of these fibers show that ZDW shifted towards longer operating wavelengths. The proposed PCFs($_{doped.2}$) showed a high effective refractive index, high negative dispersion and low confinement loss. Moreover, the dispersion profile can be compensated by its small coupling loss. The negative dispersion and low confinement loss make the proposed PCFs($_{doped.2}$) most appropriate for communication system applications. Besides, the simple circular structure makes it easier to manufacture. The empirical relation is applicable not only for PCFs of pure silica but for any doped silica, which depends on the air-filling fraction (d/Λ). Moreover, the dispersion profile varies significantly due to doping, and it can be estimated easily without any complex numerical calculation. So, it is important to conclude that the shifting of the ZDW and the

negative dispersion make the fiber valuable for broadband dispersion compensation in transmission networks, super-continuum generation and in the soliton fission.

6. Acknowledgements

The authors would like to acknowledge the Mosul University – Faculty of education for Pure Science- Department of Physics for supporting this work.

References

[1] T. A. Birks, J. C. Knight, and P. S. J. Russell, "Endlessly single-mode photonic crystal fiber," *Optics letters*, vol. 22, pp. 961-963, 1997.

[2] T. Zhang, Y. Zheng, C. Wang, Z. Mu, Y. Liu, and J. Lin, "A review of photonic crystal fiber sensor applications for different physical quantities," *Applied Spectroscopy Reviews*, vol. 53, pp. 486-502, 2018.

[3] B. M. Masum, S. M. Aminossadati, C. R. Leonardi, and M. S. Kizil, "Gas sensing with Hollow-Core Photonic Crystal Fibres: A comparative study of mode analysis and gas flow performance," *Photonics and Nanostructures-Fundamentals and Applications*, vol. 41, p. 100830, 2020.

[4] S. M. K. Alawsi, "Concentration Sensor Design Using Wavelength Shift Based Photonic Crystal Fibre," *Iraqi Journal of Science*, vol. 58, no. 4C, pp. 2496-2503, 2017.

[5] L. Zhang and C. Yang, "Photonic crystal fibers with squeezed hexagonal lattice," *Optics express*, vol. 12, pp. 2371-2376, 2004.

[6] F. F. Abbas and S. S. Ahmed, "Photonic crystal fiber pollution sensor based on surface plasmon resonance," *Iraqi Journal of Science*, pp. 658-667, 2023.

[7] P. Russell, "Photonic crystal fibers: a historical account," *IEEE Leos Newsletter*, vol. 21, pp. 11-15, 2007.

[8] W. J. Wadsworth, N. Joly, J. C. Knight, T. A. Birks, F. Biancalana, and P. S. J. Russell, "Supercontinuum and four-wave mixing with Q-switched pulses in endlessly single-mode photonic crystal fibres," *Optics express*, vol. 12, pp. 299-309, 2004.

[9] M. H. Younus, O. F. Ameen, R. K. R. Ibrahim, and N. Redzuan, "Fuel detection system using OTDR with multimode fiber," *Jurnal Teknologi*, vol. 79, no. 3, pp. ??, 2017.

[10] K. Saitoh, M. Koshiba, T. Hasegawa, and E. Sasaoka, "Chromatic dispersion control in photonic crystal fibers: application to ultra-flattened dispersion," *Optics Express*, vol. 11, pp. 843-852, 2003.

[11] N. Mortensen, M. D. Nielsen, J. R. Folkenberg, A. Petersson, and H. R. Simonsen, "Improved large-mode-area endlessly single-mode photonic crystal fibers," *Optics Letters*, vol. 28, pp. 393-395, 2003.

[12] K. Saitoh, N. Florous, and M. Koshiba, "Ultra-flattened chromatic dispersion controllability using a defected-core photonic crystal fiber with low confinement losses," *Optics Express*, vol. 13, pp. 8365-8371, 2005.

[13] A. I. Mahmood, A. I. Mahmood, and S. S. Ahmed, "Refractive Index Sensor Based on Micro-Structured Optical Fibers with Using Finite Element Method," *Iraqi Journal of Science, vol. 59. no. 3C*, pp. 1577-1586, 2018.

[14] K. Saitoh and M. Koshiba, "Numerical modeling of photonic crystal fibers," *Journal of lightwave technology*, vol. 23, p. 3580, 2005.

[15] A. Ferrando, E. Silvestre, P. Andrés, J. J. Miret, and M. V. Andrés, "Designing the properties of dispersion-flattened photonic crystal fibers," *Optics Express*, vol. 9, pp. 687-697, 2001.

[16] N. A. Mortensen, "Effective area of photonic crystal fibers," *Optics Express*, vol. 10, pp. 341-348, 2002.

[17] K. Saitoh and M. Koshiba, "Empirical relations for simple design of photonic crystal fibers," *Optics express*, vol. 13, pp. 267-274, 2005.

[18] A. Kudlinski, A. George, J. Knight, J. Travers, A. Rulkov, S. Popov, *et al.*, "Zero-dispersion wavelength decreasing photonic crystal fibers for ultraviolet-extended supercontinuum generation," *Optics Express*, vol. 14, pp. 5715-5722, 2006.

[19] K. Saitoh, M. Koshiba, and N. A. Mortensen, "Nonlinear photonic crystal fibres: pushing the zero-dispersion towards the visible," *New Journal of Physics*, vol. 8, p. 207, 2006.

[20] T.-L. Wu and C.-H. Chao, "An efficient approach for calculating the dispersions of photonic-crystal fibers: design of the nearly zero ultra-flattened dispersion," *Journal of lightwave technology,* vol. 23, p. 2055, 2005.

[21] R. K. Gangwar and V. K. Singh, "Study of highly birefringence dispersion shifted photonic crystal fiber with asymmetrical cladding," *Optik,* vol. 127, pp. 11854-11859, 2016/12/01/ 2016.

[22] T. Li, "Structures, parameters, and transmission properties of optical fibers," *Proceedings of the IEEE,* vol. 68, pp. 1175-1180, 1980.

[23] F. Karim, "Synthesis of dispersion-compensating triangular lattice index-guiding photonic crystal fibres using the directed tabu search method," *Opto-Electronics Review,* vol. 25, pp. 41-45, 2017.

[24] F. Zolla, G. Renversez, A. Nicolet, B. Kuhlmey, S. R. Guenneau, and D. Felbacq, *Foundations of photonic crystal fibres*: World Scientific, 2005.

[25] E. Grace, A. Butcher, J. Monroe, and J. A. Nikkel, "Index of refraction, Rayleigh scattering length, and Sellmeier coefficients in solid and liquid argon and xenon," *Nuclear Instruments and Methods in Physics Research Section A: Accelerators, Spectrometers, Detectors and Associated Equipment,* vol. 867, pp. 204-208, 2017.

[26] G. Ghosh, *Handbook of optical constants of solids: Handbook of thermo-optic coefficients of optical materials with applications*: Academic Press, 1998.

[27] S. K. Pandey, Y. K. Prajapati, and J. Maurya, "Design of simple circular photonic crystal fiber having high negative dispersion and ultra-low confinement loss," *Results in Optics,* vol. 1, p. 100024, 2020.